A photoreceptor cell-specific ATP-binding transporter gene (*ABCR*) is mutated in recessive Stargardt macular dystrophy

Rando Allikmets[2], Nanda Singh[3], Hui Sun[4], Noah F. Shroyer[7], Amy Hutchinson[1], Abirami Chidambaram[2], Bernard Gerrard[2], Lisa Baird[3], Dora Stauffer[3], Andy Peiffer[3], Amir Rattner[4,6], Philip Smallwood[4,6], Yixin Li[7], Kent L. Anderson[7], Richard Alan Lewis[7,8,9], Jeremy Nathans[4,5,6], Mark Leppert[3], Michael Dean[1] & James R. Lupski[7,8]

Stargardt disease (STGD, also known as fundus flavimaculatus; FFM) is an autosomal recessive retinal disorder characterized by a juvenile-onset macular dystrophy, alterations of the peripheral retina, and subretinal deposition of lipofuscin-like material. A gene encoding an ATP-binding cassette (ABC) transporter was mapped to the 2-cM (centiMorgan) interval at 1p13-p21 previously shown by linkage analysis to harbour the *STGD* gene. This gene, *ABCR*, is expressed exclusively and at high levels in the retina, in rod but not cone photoreceptors, as detected by *in situ* hybridization. Mutational analysis of *ABCR* in STGD families revealed a total of 19 different mutations including homozygous mutations in two families with consanguineous parentage. These data indicate that *ABCR* is the causal gene of STGD/FFM.

Macular degeneration is a complex disorder affecting approximately 1.7 million individuals in the U.S. and is the most common cause of acquired visual impairment in those over the age of 65 (ref.1). Stargardt disease (STGD; MIM #248200) is the most common hereditary recessive macular dystrophy (estimated incidence 1:10,000 (ref.2)) and is characterized by juvenile to young adult onset, central visual impairment, progressive bilateral atrophy of the macular retinal pigment epithelium (RPE) and neuroepithelium, with the frequent appearance of orange-yellow flecks distributed around the macula and/or the midretinal periphery[3,4]. A clinically similar retinal disorder (fundus flavimaculatus, FFM[5]) often displays later age of onset and slower progression[6,7]. From linkage analysis, it has been concluded that STGD and FFM are most likely allelic autosomal recessive disorders with slightly different clinical manifestations caused by mutation(s) of a gene at chromosome 1p13–p21 (refs 4, 8, 9). We have refined the localization of the STGD gene to a 4-cM region flanked by the recombinant markers *D1S435* and *D1S236* and constructed a complete YAC contig of the region. Recently, the location of the STGD/FFM locus on human chromosome 1p has been refined to a 2-cM interval between polymorphic markers *D1S406* and *D1S236* by genetic linkage analysis in an independent set of STGD families[10]. Autosomal dominant disorders with somewhat similar clinical phenotypes to STGD, identified in single large North American pedigrees, have been mapped to chromosome 13q34 (STGD2; MIM #153900; ref.11) and to chromosome 6q11–q14 (STGD3; MIM #600110; ref.12), although these conditions are not characterized by the pathognomonic dark choroid observed by fluorescein angiography[13].

We have been characterizing the superfamily of mammalian ABC transporters and mapping its members as possible candidates for human disease phenotypes. The ABC superfamily includes genes whose products are transmembrane proteins involved in energy-dependent transport of a wide spectrum of substrates across membranes[14,15]. Many disease-causing members of this superfamily result in defects in the transport of specific substrates (CFTR[16]; ALD[17]; SUR[18]; PMP70[19]; TAP+2[20]). In eukaryotes, ABC genes typically encode four domains that include two conserved ATP-binding domains (ATP) and two domains with multiple transmembrane (TM) segments[21]. The ATP-binding domains of ABC genes contain motifs of characteristic conserved residues (Walker A and B motifs) spaced by 90–120 amino acids. Both this conserved spacing and the 'Signature' or 'C' motif just upstream of the Walker B site distinguish members of the ABC superfamily from other ATP-binding proteins[21,22]. These features have allowed us to isolate new ABC genes by hybridization, degenerate PCR, and inspection of DNA sequence databases[23–26].

Recently, we characterized 21 new members of the ABC superfamily and have begun to assign functions to these genes by determining their map locations and their patterns of expression[27]. That many known ABC genes are involved in inherited human diseases suggests that some of these new loci will also encode proteins mutated in specific genetic disorders. Here we describe a retina-specific ABC transporter and its role in the recessive macular dystrophy, STGD/FFM.

Identification of the *ABCR* as a candidate gene for STGD

We identified one of the 21 new human genes from the ABC superfamily[27], hereafter called *ABCR* (retina-specific ABC transporter), among expressed sequence tags (ESTs) obtained from 5,000 human retina cDNA clones (J.P. Macke, P.S., J.N., unpublished) and among ESTs obtained from human retina cDNA clones by the I.M.A.G.E.

[1]*Laboratory of Genomic Diversity,* [2]*Intramural Research Support Program, SAIC-Frederick, National Cancer Institute-Frederick Cancer Research and Development Center, Frederick, Maryland 21702-1201, USA.* [3]*Department of Human Genetics, University of Utah, Salt Lake City, Utah 84112, USA. Departments of* [4]*Molecular Biology and Genetics,* [5]*Neuroscience, and Ophthalmology,* [6]*Howard Hughes Medical Institute, Johns Hopkins University School of Medicine, Baltimore, Maryland 21205, USA. Departments of* [7]*Molecular and Human Genetics,* [8]*Pediatrics,* [9]*Ophthalmology, and Medicine, Baylor College of Medicine, Houston, Texas 77030, USA. Correspondence should be addressed to: M.D. e-mail: dean@fcrfv1.ncifcrf.gov*

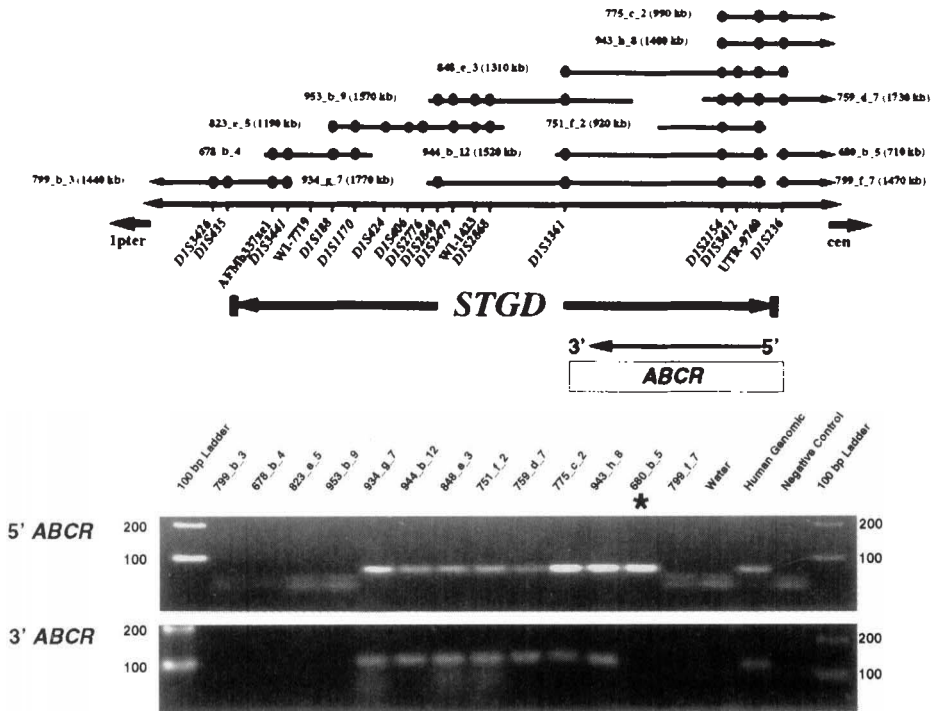

Fig. 1 Physical mapping of the *ABCR* gene. Mega-YAC clones from the CEPH mega-YAC genomic library[76] encompassing the 4-cM critical region for STGD are represented by horizontal bars with shaded circles indicating confirmed positives for STSs by landmark mapping. The individual STS markers and their physical order are shown below the YACs with arrows indicating the centromeric (cen) and telomeric (1pter) direction[4]. The horizontal double head arrow labelled *STGD* indicates the refined genetic interval delineated by historical recombinants[4]. Below are results of agarose gel electrophoresis of PCR amplification products with primers from the 5' (5'–GGTCTTCGTGTGTGGTCATT–3', 5'–GGTCCAGTTCTTCCAGAG–3', labelled 5' *ABCR*) or 3' (5'–ATCCTCTGACTCAGCAATCACA–3', 5'–TTGCAATTACAAATGCAATGG–3', labelled 3' *ABCR*) regions of *ABCR* on the 13 different YAC DNA templates indicated as diagonals above the gel. The asterisk denotes that YAC 680_b_5 was positive for the 5' *ABCR* PCR but negative for the 3' *ABCR* PCR. These data suggest the *ABCR* gene maps within the interval delineated by markers *D1S3361–D1S236* and is transcribed toward the telomere, as depicted by the open horizontal box.

consortium[28]. *ABCR* is closely related to the described mouse and human *ABC1* and *ABC2* genes[24,26]. To determine whether *ABCR* might cause a disease phenotype, we mapped the gene with a whole genome radiation hybrid panel (GeneBridge 4; Research Genetics). *ABCR* mapped to the human chromosome 1p13–p21 region, close to microsatellite markers *D1S236* and *D1S188*. To define further the location of the gene, we used PCR primers from the putative 3' untranslated region to screen YACs from the described contig between these anonymous markers[4]. At least 12 YACs contain the 3' end of the *ABCR* gene, including 924_e_9, 759_d_7, 775_c_2, 782_b_4, 982_g_5, 775_b_2, 765_a_3, 751_f_2, 848_e_3, 943_h_8, 934_g_7, and 944_b_12 (Fig. 1). These YACs delineate a region containing the *STGD* gene between markers *D1S3361* and *D1S236* (for a more detailed map of the region, see ref. 4).

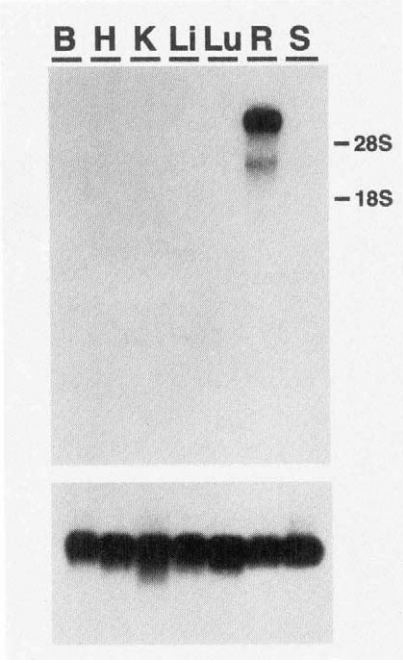

Fig. 2 Size and tissue distribution of *Abcr* transcripts in the adult rat. Blot of total RNA from the indicated tissues was hybridized with a 1.6-kb mouse *Abcr* probe (top) or a ribosomal protein S26 probe[77] (bottom). The *ABCR* probe revealed a predominant transcript of approximately 8 kb that is found in retina only. The mobility of the 28S and 18S ribosomal RNAs are indicated at the right. B, brain; H, heart; K, kidney; Li, liver; Lu, lung; R, retina; S, spleen.

Expression of the *ABCR* gene

Our expression studies and inspection of the EST databases added further support that *ABCR* is the candidate *STGD* gene. Hybridization of a 3' *ABCR* cDNA probe to a multiple tissue northern blot and a MasterBlot indicated that the gene was not expressed detectably in any of the 50 non-retinal fetal and adult tissues we examined (data not shown), consistent with our observation that all 12 of the *ABCR* clones in the EST database originated from retinal cDNA libraries. Furthermore, when we screened cDNA libraries from both developing mouse eye and adult human retina with *ABCR* probes we found a high frequency of *ABCR* clones, estimated at 0.1%-1% of all cDNA clones in the library. Hybridization of the *ABCR* probe to a northern blot containing total RNA from rat retina and other tissues showed that the expression of this gene is uniquely retina-specific (Fig. 2). The transcript size is estimated to be 8 kb.

Sequence and exon/intron structure of the *ABCR* cDNA

We used several ESTs that were derived from retina cDNA libraries and had high similarity to the mouse *Abc1* gene to facilitate the assembly of most of the *ABCR* cDNA sequence. We linked the retina cDNA clones by RT-PCR, and repetitive screening of a human retina cDNA library with 3' and 5' PCR probes together with 5' RACE to characterize the terminal sequences of the gene. We assembled a total of 7.1 kb of the *ABCR* sequence (Fig. 3) resulting in a 6,705-bp (2,235-amino acid) open reading frame.

Screening of a bacteriophage λ human genomic library with cDNA probes yielded a contig that spans approximately 100 kb and contains the entire *ABCR* coding region (data not shown). We characterized the exon/intron structure of 36 exons of the gene (corresponding to residues 652–2235) by direct sequencing of genomic and cDNA clones. Primers used for amplification of individual exons are shown in Table 2. We estimated the intron sizes

Fig. 3 Below ▼ and opposite page. ▶ Sequence of the *ABCR* coding region. The sequence of the *ABCR* cDNA is shown with the predicted protein sequence in one-letter amino acid code below. The location of the splice sites identified starting from nucleotide 2161 is shown by the symbol I. Transmembrane domains predicted by hydropathy plot are underlined, the ATP-binding domains are in bold type and the termination codon is indicated with an asterisk. The location of missense mutations and the in-frame deletion are shown below the sequence.

```
-80  CTGGCTCTTAACGGCGTTTATGTCCTTTGCTGTCTGAGGGGCCTCAGCTCTGACCAATCTGGTCTTCGTGTGGTCATTAGCATGGGCTTCGTGAGACAGATACAGCTTTTCCTCTGGAAG
-26                                                                                                                  M  G  F  V  R  Q  I  Q  L  L  L  W  K

 40  AACTGGACCCTGCGGAAAAGGCAAAAGATTCGCTTTGTGGTGGAACTCGTGTGGCCTTTATCTTTATTTCTGGTCTTGATCTGGTTAAGGAATGCCAACCCGCTCTACAGCCATCATGAA
 14  N  W  T  L  R  K  R  Q  K  I  R  F  V  V  E  L  V  W  P  L  S  I  F  L  V  L  I  W  L  R  N  A  N  P  L  Y  S  H  H  E

160  TGCCATTTCCCCAACAAGGCGATGCCCTCAGCAGGAATGCTGCCGTGGCTCCAGGGGATCTTCTGCAATGTGAACAATCCCTGTTTTCAAAGCCCCACCCCAGGAGAATCTCCTGGAATT
 54  C  H  F  P  N  K  A  M  P  S  A  G  M  L  P  W  L  Q  G  I  F  C  N  V  N  N  P  C  F  Q  S  P  T  P  G  E  S  P  G  I

280  GTGTCAAACTATAACAACTCCATCTTGGCAAGGGTATATCGAGATTTTCAAGAACTCCTCATGAATGCACCAGAGAGCCAGCACCTTGGCCCTATTTGGACAGACCTACACATCTTGTCC
 94  V  S  N  Y  N  N  S  I  L  A  R  V  Y  R  D  F  Q  E  L  L  M  N  A  P  E  S  Q  H  L  G  R  I  W  T  E  L  H  I  L  S

400  CAATTCATGGACACCCTCCGGACTCACCCGGAGAGAATTGCAGGAAGAGGAATACGAATAAGGGATATCTTCAAAGATGAAGAAACACTGACACTATTTCTCATTAAAAACATCGGCCTG
134  Q  F  M  D  T  L  R  T  H  P  E  R  I  A  G  R  G  I  R  I  R  D  I  L  K  D  E  E  T  L  T  I  F  L  I  K  N  I  G  L

520  TCTGACTCAGTGGTCTACCTTCTGATCAACTCTCAAGTCCGTCCAGAGCAGTTCGCTCATGGAGTCCCGGACCTGGCGCTGAAGGACATCGCCTGCAGCGAGGCCCTCCTGGAGCGCTTC
174  S  D  S  V  V  Y  L  L  I  N  S  Q  V  R  P  E  Q  F  A  H  G  V  P  D  L  A  L  K  D  I  A  C  S  E  A  L  L  E  R  F

640  ATCATCTTCAGCCAGAGACGCGGGGCAAAGACGGTGCGCTATGCCCTGTGCTCCCTCTCCAGGGCACCCTACACTGGATAGAAGACACTCTGTATGCCAACGTGGACTTCTTCAAGCTC
214  I  I  F  S  Q  R  R  G  A  K  T  V  R  Y  A  L  C  S  L  S  Q  G  T  L  Q  W  I  E  D  T  L  Y  A  N  V  D  F  F  K  L

760  TTCCGTGTGCTTCCCACACTCCTAGACAGCCGTTCTCAAGGTATCAATCTGAGATCTTGGGGAGGAATATTATCTGATATGTCACCAAGAATTCAAGAGTTTATCCATCGGCCGAGTATG
254  F  R  V  L  P  T  L  L  D  S  R  S  Q  G  I  N  L  R  S  W  G  G  I  L  S  D  M  S  P  R  I  Q  E  F  I  H  R  P  S  M

880  CAGGACTTGCTGTGGGTGACCAGGCCCCTCATGCAGAATGGTGGTCCAGAGACCTTTACAAAGCTGATGGGCATCCTGTCTGACCTCCTGTGTGGCTACCCCGAGGGAGGTGGCTCTCCG
294  Q  D  L  L  W  V  T  R  P  L  M  Q  N  G  G  P  E  T  F  T  K  L  M  G  I  L  S  D  L  L  C  G  Y  P  E  G  G  G  S  R

1000 GTGCTCTCCTTCAACTGGTATGAAGACAATAACTATAAGGCCTTTCTGGGGATTGACTCCACAAGGAAGGATCCTATCTACTCTTATGACAGAAGAACAACATCCTTTTGTAATGCATTG
334  V  L  S  F  N  W  Y  E  D  N  N  Y  K  A  F  L  G  I  D  S  T  R  K  D  P  I  Y  S  Y  D  R  R  T  T  S  F  C  N  A  L

1120 ATCCAGAGCCTGGAGTCAAATCCTTTAACCAAAATCGCTTGGAGGGCGGCAAAGCCTTTGCTGATGGGAAAAATCCTGTACACTCCTGATTCACCTGCAGCACGAAGGATACTGAAGAAT
374  I  Q  S  L  E  S  N  P  L  T  K  I  A  W  R  A  A  K  P  L  L  M  G  K  I  L  Y  T  P  D  S  P  A  A  R  R  I  L  K  N

1240 GCCAACTCAACTTTTGAAGAACTGGAACACGTTAGGAAGTTGGTCAAAGCCTGGGAAGAAGTAGGGCCCCAGATCTGGTACTTCTTTGACAACAGCACACAGATGAACATGATCAGAGAT
414  A  N  S  T  F  E  E  L  E  H  V  R  K  L  V  K  A  W  E  E  V  G  P  Q  I  W  Y  F  F  D  N  S  T  Q  M  N  M  I  R  D

1360 ACCCTGGGGAACCCAACAGTAAAAGACTTTTTGAATAGGCAGCTTGGTGAAGAAGGTATTACTGCTGAAGCCATCCTAAACTTCCTCTACAAGGGCCCTCGGGAAAGCCAGGCTGAGGAC
454  T  L  G  N  P  T  V  K  D  F  L  N  R  Q  L  G  E  E  G  I  T  A  E  A  I  L  N  F  L  Y  K  G  P  R  E  S  Q  A  E  D
1480 ATGGCCAACTTCGACTGGAGGGACATATTTAACATCACTGATCGCACCCTCCGCCTGGTCAATCAATACCTGGAGTGCTTGGTCCTGGATAAGTTTGAAAGCTACAATGATGAAACTCAG
494  M  A  N  F  D  W  R  D  I  F  N  I  T  D  R  T  L  R  L  V  N  Q  Y  L  E  C  L  V  L  D  K  F  E  S  Y  N  D  E  T  Q

1600 CTCACCCAACGTGCCCTCTCTCTACTGGAGGAAAACATGTTCTGGGCCGGAGTGGTATTCCCTGACATGTATCCCTGGACCAGCTCTCTACCACCCCACGTGAAGTATAAGATCCGAATG
534  L  T  Q  R  A  L  S  L  L  E  E  N  M  F  W  A  G  V  V  F  P  D  M  Y  P  W  T  S  S  L  P  P  H  V  K  Y  K  I  R  M

1720 GACATAGACGTGGTGGAGAAAACCAATAAGATTAAAGACAGGTATTGGGATTCTGGTCCCAGAGCTGATCCCGTGGAAGATTTCCGGTACATCTGGGGCGGGTTTGCCTATCTGCACGAC
574  D  I  D  V  V  E  K  T  N  K  I  K  D  R  Y  W  D  S  G  P  R  A  D  P  V  E  D  F  R  Y  I  W  G  G  F  A  Y  L  C  D

1840 ATGGTTGAACAGGGGATCACAAGGAGCCAGGTGCAGGCGGAGGCTCCAGTTGGAATCTACCTCCAGCAGATGCCCTACCCCTGCTTCGTGGACGATTCTTTCATGATCATCCTGAACCGC
614  M  V  E  Q  G  I  T  R  S  Q  V  Q  A  E  A  P  V  G  I  Y  L  Q  Q  M  P  Y  P  C  F  V  D  D  S  F  M  I  I  L  N  R

1960 TGTTTCCCTATCTTCATGGTGCTGGCATGGATCTACTCTGTCTCCATGACTGTGAAGAGCATCGGTCTTGGAGAAGGAGTTGCGACTGaAGGAGACCTTCAAAAATCAGGGTGTCTCGAAT
654  C  F  P  I  F  M  V  L  A  W  I  Y  S  V  S  M  T  V  K  S  I  V  L  E  K  E  L  R  L  K  E  T  L  K  N  Q  G  V  S  N

2080 GCAGTGATTTGGTGTACCTGGTTCCTGGACAGCTTCTCCATCATGTCGATGAGCATCTTCCTCCTGACGATATTCATCATG1CATGGAAGAATCCTACATTACAGCGACCCATTCATCCTC
694  A  V  I  W  C  T  W  F  L  D  S  F  S  I  M  S  M  S  I  F  L  L  T  I  F  I  M  H  G  R  I  L  H  Y  S  D  P  F  I  L

2200 TTCCTGTTCTTGTTGGCTTTCTCCACTGCCACCATCATGCTGTGCTTTCTGCTCAGCACCTTCTTCTCCAAGGCCAGTCTGGCAGCAGCCTGTAGTGGTGTCATCTATTTCACCCTCTAC
734  F  L  F  L  L  A  F  S  T  A  T  I  M  L  C  F  L  L  S  T  F  F  S  K  A  S  L  A  A  A  C  S  G  V  I  Y  F  T  L  Y

2320 CTGCCACACATCCTGTGCTTCGCCTGGCAGGACCGCATGACCGCTGAGCTGAAGAAGGCTGTG1AGCTTACTGTCTCCGGTGGCATTTGGATTTGGCACTGAGTACCTGGTTCGCTTCGAA
774  L  P  H  I  L  C  F  A  W  Q  D  R  M  T  A  E  L  K  K  A  V  S  L  L  S  F  V  A  F  G  F  G  T  E  Y  L  V  R  F  E

2440 GAGCAAGGCCTGGGGCTGCAGTGGAGCAACATCGGGAACAGTCCCACGGAAGGGGACGAATTCAGCTTCCTGCTGTCCATGCAGATGATGCTCCTTGATGCTGCGTGCTATGGCTTACTC
814  E  Q  G  L  G  L  Q  W  S  N  I  G  N  S  P  T  E  G  D  E  F  S  F  L  L  S  M  Q  M  M  L  L  D  A  A  C  Y  G  L  L
                G618E
2560 GCTTGGTACCTTGATCAGGTGTTTCCAG1GAGACTATGGAACCCCACTTCCTTGGTACTTTCTTCTACAAGAGTCGTATTGGCTTAGCGGTGAAG1GGTGTTCAACCAGAGAAGAAAGAGCC
854  A  W  Y  L  D  Q  V  F  P  G  D  Y  G  T  P  L  P  W  Y  F  L  I  Q  E  S  Y  W  L  S  G  E  G  C  S  T  R  E  E  R  A
                      G863A
2680 CTGGAAAAGACCGAGCCCCTAACAGAGGAAACGGAGGATCCAGAGCACCCAGAAGGAATACAC1GACTCCTTCTTTGAACGTGAGCATCCAGGGTGGGTTCCTGGGGTATGCGTGAAGAAT
894  L  E  K  T  E  P  L  T  E  E  T  E  D  P  E  H  P  E  G  I  H  D  S  F  F  E  R  E  H  P  G  W  V  P  G  V  C  V  K  N
                                                                                                                  V931M

2800 CTGGTAAAGATTTTTGAGCCCTGTGGCCGGCCAGCTGTGGACCGTCTGAACATCACCTTCTACGAGAACCAGATCACCGCATTCCTGGGCCACAATGGAGCTGGGAAAACCACCACCTTGT
934  L  V  K  I  F  E  P  C  G  R  P  A  V  D  R  L  N  I  T  F  Y  E  N  Q  I  T  A  F  L  G  H  W  G  A  G  K  T  T  T  L
2920 TCCATCCTGACGGGTCTGTTGCCACCAACCTCTGGGACTGTGCTCGTTGGGGGAAGGGACATTGAAACCAGCCTGGATGCAGTCCGGCAGAGCCTTGGCATGTGTCCACAGCACAACATC
974  S  I  L  T  G  L  L  P  P  T  S  G  T  V  L  V  G  G  R  D  I  E  T  S  L  D  A  V  R  Q  S  L  G  M  C  P  Q  H  N  I

3040 CTGTTCCACCA1CCTCACGGTGGCTGAGCACATGCTGTTCTATGCCCAGCTGAAAGGAAAGTCCCAGGACGAGGCCCAGCTGGAGATGGAAGCCATGTTGGAGGACACAGGCCTCCACCAC
1014 L  F  H  H  L  T  V  A  E  H  M  L  F  Y  A  Q  L  K  G  K  S  Q  E  E  A  Q  L  E  M  E  A  M  L  E  D  T  G  L  H  H
                                A1028V
3160 AAGCGGAATGAAGAGGCTCAGGACCTAT1CAGGTGGCATGCAGAGAAAGCTGTCGGTTGCCATTGCCTTTGTGGGAGATGCCAAGGTGGTGATTCTGGACGAACCCACCTCTGGGGTGGAC
1054 K  R  N  E  E  A  Q  D  L  S  G  G  M  Q  R  K  L  S  V  A  I  A  F  V  G  D  A  K  V  V  I  L  D  E  P  T  S  G  V  D
                                                V1072A                                                E1087K
3280 CCTTACTCGAGACGCTCAATCTGGGATCTGCTCCTGAAGTATCGCTCAG1GCAGAACCATCATCATGCCCACTCACCACATGGACGAGGCCGACCACCAAGGGGACCGCATCGCCATCATT
1093 P  Y  S  R  R  S  I  W  D  L  L  L  K  Y  R  S  G  R  T  I  I  M  P  T  H  H  M  D  E  A  D  H  Q  G  D  R  I  A  I  I

3400 GCCCAGGGAAGGCTCTACTGCTCAGGCACCCCACTCTTCCTGAAGAACTGCTTTGGCACAGGCTTGTACTTAACCTTGGTGCGCAAGATGAAAAACATCCAGAGCCAAACGAAAGGCAGT
1134 A  Q  G  R  L  Y  C  S  G  T  P  L  F  L  K  N  C  F  G  T  G  L  Y  L  T  L  V  R  K  M  K  N  I  Q  S  Q  R  K  G  S

3520 GAG1GGGACCTGCAGCTGCTCGTCTAAGGGTTTCTCCACCACGTGTCCAGCCCACGTCGATGACCTAACTCCAGAACAAGTCCTGGAT1GGGGATGTAAATGAGCTGATCGATGTAGTCCTG
```

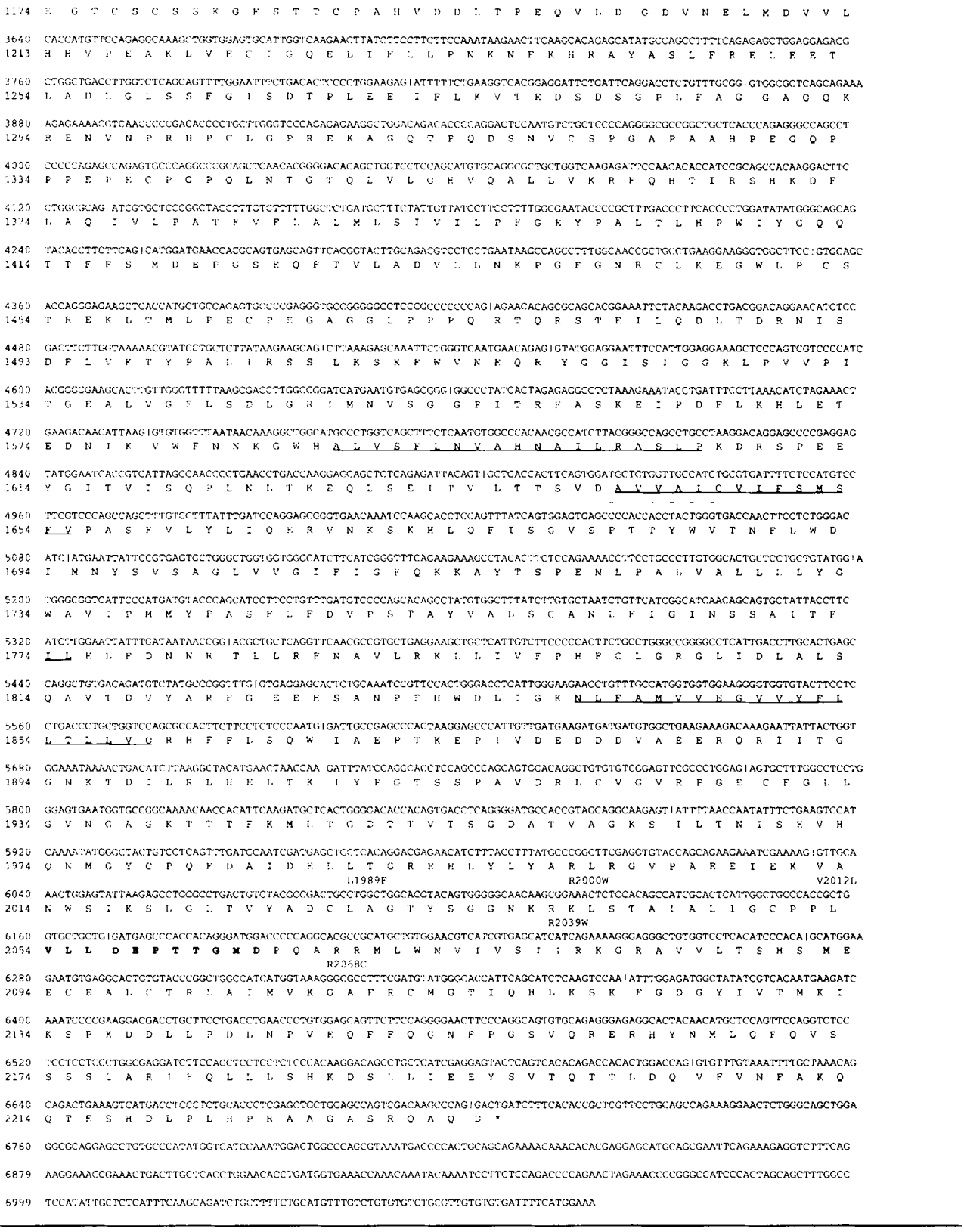

from the sizes of PCR products generated using primers from adjacent exons with genomic phage clones as templates.

Homology to ABC superfamily members

We performed a BLAST search and revealed that *ABCR* is most closely related to the characterized mouse *Abc1* and *Abc2* genes[26] and to another human gene (*ABCC*) which maps to chromosome 16p13.3 (ref. 29). These genes, together with *ABCR* and a gene from *C. elegans* (GenBank #Z29117), form a subfamily of genes specific to multicellular organisms and not represented in yeast[22,27]. Alignment of the cDNA sequence of *ABCR* with the *Abc1*, *Abc2*, and *ABCC* genes revealed, as expected, the highest

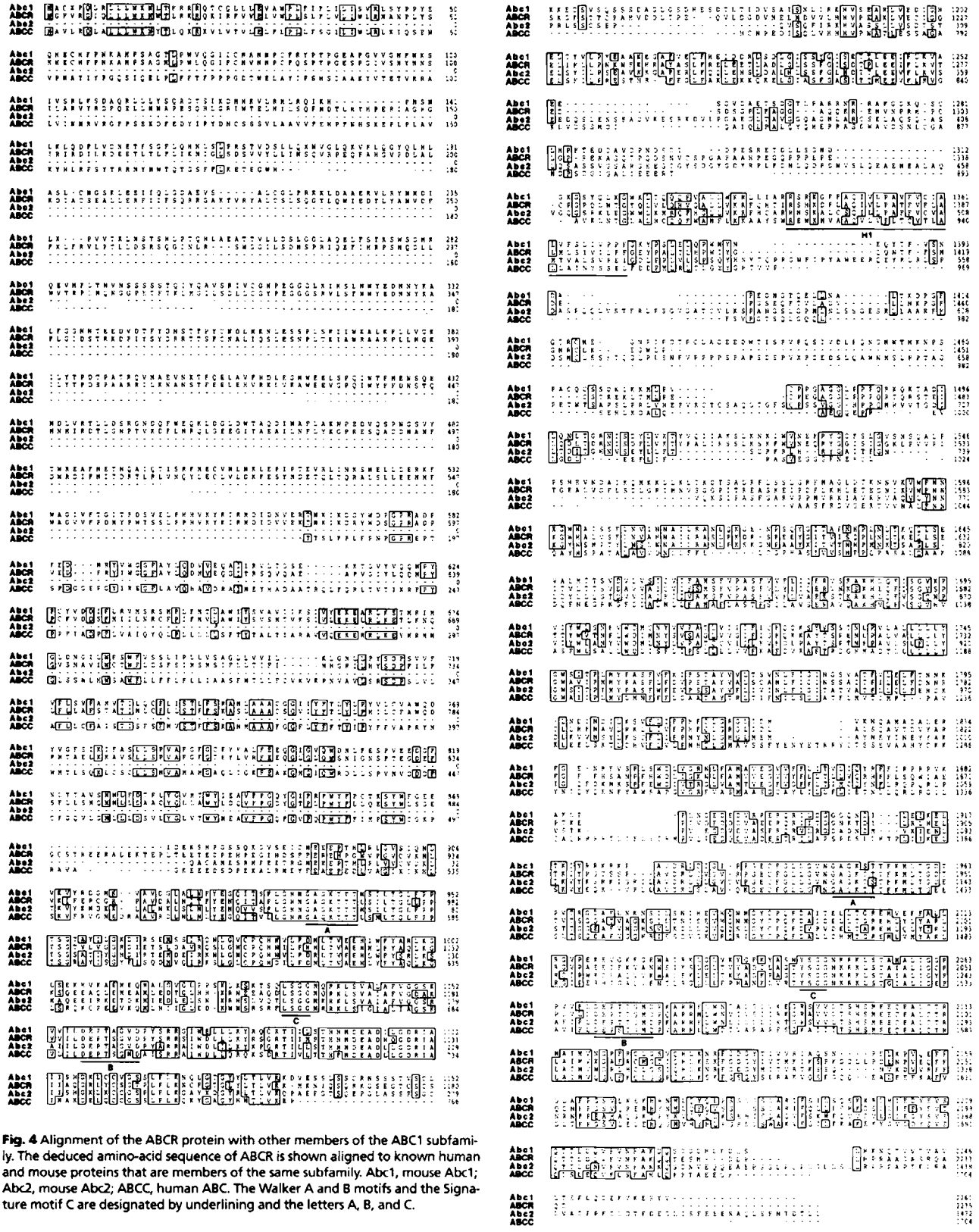

Fig. 4 Alignment of the ABCR protein with other members of the ABC1 subfamily. The deduced amino-acid sequence of ABCR is shown aligned to known human and mouse proteins that are members of the same subfamily. Abc1, mouse Abc1; Abc2, mouse Abc2; ABCC, human ABC. The Walker A and B motifs and the Signature motif C are designated by underlining and the letters A, B, and C.

degree of homology within the ATP-binding cassettes. The predicted amino-acid identity of the *ABCR* gene to mouse *Abc1* was 70% within the ATP-binding domains; even within hydrophobic membrane-spanning segments, identity ranged between 55 and 85% (Fig. 4). The putative *ABCR* initiator methionine (Figs 3, 4) corresponds to a methionine codon at the 5' end of *Abc1* (ref. 26). Considerable identity is observed in the first 45 amino acids of *ABCR*, *Abc1*, and *ABCC*.

Table 1 • Mutations and polymorphisms in the *ABCR* gene in STGD families

Mutation	Exon/Nucl.	# families	Con.	Nucl. change	Comment
G818E	2383	1	100	G2453A	
G863A	2383	3	100	G2588C	AR-128[c]
V931M	2743	1	80	G2791A	KKESH-214[a]
2884delC	2743	1	80	frameshift	
N965M	2743	1	80	A2893G	AR-128[b]
A1028V	3051	5	140	C3083T	AR-71[c], AR-181[c]
3211insGT	3188	1	80	frameshift	
V1072A	3188	1	80	T3216C	
E1087K	3188	1	80	G3259A	
4730delC	4735	1	100	frameshift	
ΔVVAIC1643	4905	1	170	4927del15	AR-293[a]
5082+2T→C	4905	1	170	splice donor site	AR-71[b]
5892+1G→T	5783	1	80	splice donor site	
L1989F	5893	3	80	C5965T	AR-181[b]
R2000W	5893	1	80	C5998T	
V2012L	6034	2	80	G6034C	
R2039W	6034	1	80	C6115T	
R2068C	6169	1	80	C6202T	AR-280[c]
6595insG	6366	1	80	frameshift	AR-280[b]
Polymorphisms					
D847H	2383	1	100	G2636C	0.02
R943Q	2743	4	80	G2829A	0.06
I1985I	5893	5	80	C5955T	0.08
I2045I	6034	6	80	C6145T	0.10
V2056V	6169	1	16	G6228A	0.00

Mutations are named according to standard nomenclature. Exon/Nucl., exon numbering according to the nucleotide position starting from the A in the initiator ATG. Con., the number of control chomosomes tested for each missense alteration. The comment field indicates compound heterozygous families, in which 2 independent altered alleles were identified, and homozygous families. For polymorphisms the observed frequency of the rare allele in control chromosomes is shown. [a]Consanguineous patients homozygous for the alteration. [b]Maternally inherited mutation. [c]Paternally inherited mutation.

ABCR shows the composition of a typical full-length ABC transporter that consists of two transmembrane domains (TM), each with six membrane spanning hydrophobic segments, as predicted by a hydropathy plot (data not shown), and two highly conserved ATP-binding domains (Figs 3, 4). In addition, the HH1 hydrophobic domain, located between the first ATP and second TM domain and specific to this subfamily[26], showed a predicted 57% amino acid identity (24/42 aa) with the mouse *Abc1* gene.

To characterize the mouse orthologue of *ABCR*, we isolated cDNA clones from a developing mouse eye library. We utilized a partial sequence from the mouse cDNA to design PCR primers to map the mouse *Abcr* gene in an interspecific backcross mapping panel (Jackson BSS). The allele pattern of *Abcr* was compared to 2,450 other loci mapped in the Jackson BSS cross; we found linkage to the distal end of chromosome 3 (Fig. 5). We observed no recombinants between *Abcr* and *D13Mit13*. This region of the mouse genome is syntenic with human chromosome 1p13-p21. Thus far, no eye disease phenotype has been mapped to this region of mouse chromosome 3.

Compound heterozygous and homozygous mutations in STGD patients

We pursued mutational analysis of the *ABCR* gene in 48 STGD families previously ascertained by strict definitional criteria and shown to be linked to chromosome 1p[4,30]. So far, we have used a total of 21 exons for the mutation analyses. A total of 19 different mutations was identified, the majority representing missense mutations in conserved amino acid positions. However, we also found several 1–2-bp insertions and deletions representing frameshifts (Table 1). Two missense alterations were found (D847H, R943Q) in at least one control individual, suggesting that they are neutral polymorphisms. We only found the remaining mutations in STGD patients and not in at least 40 unrelated normal controls (80 chromosomes), consistent with the interpretation that these alterations represent disease-causing mutations, not polymorphisms. One of the mutations, 5892+1 G→T, occurs in family AR144 in which one of the affected children is recombinant for the flanking marker *D1S236* (ref. 4). This mutation, however, is present in the father as well as in both affected children. Therefore, the *ABCR* gene is non-recombinant with respect to the STGD locus.

The mutations are scattered throughout the coding sequence of the *ABCR* gene (see Table 1; Fig. 3), although clustering within the conserved regions of the ATP-binding domains is noticeable. We detected homozygous mutations in two likely consanguineous families, one Saudi Arabian (KKESH214) and one North American (AR293; ref.4), in each of which only the affected individuals inherited the identical disease allele (Table 1; Fig. 6). We identified four compound heterozygous families where the two disease alleles were transmitted from different parents to only the affected offspring (AR71, AR128, AR181, AR280; Table 1).

In situ hybridization

STGD is characterized histologically by a massive accumulation of a lipofuscin-like substance in the retinal pigment epithelium (RPE). This characteristic has led to the suggestion that STGD represents an RPE storage disorder[2]. It was therefore of interest that we found *ABCR* transcripts to be abundant in the retina. To identify the site(s) of *ABCR* gene expression at higher resolution and to determine whether the gene is also expressed in the RPE, we visualized the distribution of *ABCR* transcripts by *in situ* hybridization to mouse, rat, bovine, and macaque ocular tissues. These experiments showed that *ABCR* transcripts are present exclusively within photoreceptor cells (Fig. 7). *ABCR* transcripts are localized principally to the rod inner segments, a distribution that closely matches that of rhodopsin gene transcripts. Interestingly, we did not observe *ABCR* hybridization at detectable levels in cone photoreceptors, as judged by comparisons with the hybridization patterns obtained with a blue cone pigment probe (compare Figs. 7*a* with *d*, 7*e* with *f* and 7*g* with *h*). Because melanin granules might obscure a weak hybridization signal in the RPE of a pigmented animal, we also examined the distribution of *ABCR* transcripts in both albino rats and albino mice. In these experiments, the *ABCR* hybridization signal was seen in the photoreceptor inner segments and was unequivocally absent from the RPE (Fig. 7*e*, data not shown). Given that *ABCR* transcripts in each of these mammals, including a primate, are photoreceptor-specific, it is highly likely that the distribution of *ABCR* transcripts conforms to this pattern as well in the human retina.

Discussion

***ABCR* and the ABC family of transporters.** We describe a retina-specific ABC transporter (*ABCR*) that is mutated in patients with the recessive macular dystrophy, STGD/FFM. *ABCR* is a member of the subfamily of ABC transporters that contain a complete transporter structure (two ATP-binding cassettes and two domains of six predicted transmembrane segments) within a single polypeptide chain. Among the known ABC transporters, *ABCR* is most closely related to the *Abc1* and *Abc2* genes. *Abc1* is highly expressed in macrophages and has been associated with the scavenging of apoptotic cells[31]. The human *ABC2* gene is expressed

Table 2 • Exon/intron primers for *ABCR*

Exon/Nucl.	Primer	Sequence
2161	12FOR	5'–AGGCTGGTGGGAGAGAGC–3'
	12REV	5'–AGTGGACCCCCTCAGAGG–3'
2383	13FOR	5'–CTGTTGCATTGGATAAAAGGC–3'
	13REV	5'–GATGAATGGAGAGGGCTGG–3'
2588[a]	ExonJ-FOR	5'–CTGCGGTAAGGTAGGATAGGG–3'
	ExonJ-REV	5'–CACACCGTTTACATAGAGGGC–3'
2654[a]	ExonK-FOR	5'–CTCTCCCCTCCTTTCCTG–3'
	ExonK-REV	5'–GTCAGTTTCCGTAGGCTTC–3'
2743	15FOR	5'–TGGGGCCATGTAATTAGGC–3'
	15REV	5'–TGGGAAAGAGTAGACAGCCG–3'
2920	2R3NFOR	5'–ACTGAACCTGGTGTGGGG–3'
	2F3REV	5'–TATCTCTGCCTGTGCCCAG–3'
3051	2R5NFOR	5'–GTAAGATCAGCTGCTGGAAG–3'
	2F4NREV	5'–GAAGCTCTCCTGCTCCAAGC–3'
3188	2F5RFOR2	5'–AGGTACCCCCACAATGCC–3'
	2F5REV	5'–TCATTGTGGTTCCAGTACTCAG–3'
3329	2R6FOR	5'–TTTTTGCAACTATATAGCCAGG–3'
	2F6REV	5'–AGCCTGTGTGAGTAGCCATG–3'
3523	2F7RFOR	5'–GCATCAGGGAGAGGCTGTC–3'
	2F7REV	5'–CCCAGCAATACTGGGAGATG–3'
3607	2R11FOR	5'–GGTAACCTCACAGTCTTCC–3'
	23F1REV	5'–GGGAACGATGGCTTTTTGC–3'
3863	23R3FOR	5'–GCTACCAGCCTGGTATTTCATTG–3'
	23F3REV	5'–GTTATAACCCATGCCTGAAG–3'
4554	33G1FOR	5'–TTCATGTTTCCCTACAAAACCC–3'
	33G1REV	5'–CATGAGAGTTTCTCATTCATGG–3'
4660[a]	ExonA-FOR	5'–GCTTAACTACCATGAATGAG–3'
	ExonA-REV	5'–ATTCCTTGCTAGATTTCAGC–3'
4735[a]	ExonB-FOR	5'–GCAGCGTCTCAGATGTCCTC–3'
	ExonB-REV	5'–AAGAGTGGAGAAGGTGACAAG–3'
4905[a]	ExonF-FOR	5'–ATATGGGTGCTGTTGCATTG–3'
	ExonF-REV	5'–TAGAGGAGGATGCTTACCTGG–3'
5783	4RXFOR	5'–CTTACCCTGGGGCCTGAC–3'
	4F4NNREV	5'–CTCAGAGCCACCCTACTATAG–3'
5893	62R4FOR	5'–GAAGCTTCTCCAGCCCTAGC–3'
	62R3REV	5'–TGCACTCTCATGAAACAGGC–3'
6034	4R5FOR	5'–GTTTGGGGTGTTTGCTTGTC–3'
	4R5REV	5'–ACCTATTTCCCCAACCCAAGAG–3'
6169	E1RFOR	5'–GAAGCAGTAATCAGAAGGGC–3'
	E1FREV	5'–GCCTCACATTCTTCCATGCTG–3'
6366	E2RFOR	5'–ATTACCTTAGGCCCAACCAC–3'
	E3FREV	5'–ACACTGGGTGTTCTGGACC–3'

PCR conditions were 95 °C, 8 min; 5 cycles of 62 °C, 20 s, 72 °C, 30 s; 35 cycles of 60 °C, 20 s, 72 °C, 30 s; 72 °C, 5 min. [a]PCR conditions were 94 °C, 5 min; 35 cycles 94 °C, 40 s; 56 °C, 30 s; 72 °C, 20 s; 72 °C, 5 min.

primarily in the brain; its function is at present unknown[24]. Another human *Abc1*-related gene that is expressed ubiquitously has also been characterized[27,29]. This subfamily of ABC transporters is not represented by any homologue in yeast[22], suggesting that these genes evolved to perform specialized functions in multicellular organisms.

ABCR and photoreceptor function. *ABCR* transcripts are abundant in the retina, suggesting that the corresponding protein is also abundant in this tissue. We localized the *ABCR* mRNA to rod photoreceptor cells by *in situ* hybridization, which implies a highly specific function for this transporter protein. Interestingly, we did not detect *ABCR* transcripts in cone photoreceptors, suggesting that a different gene product may perform the corresponding function in cones.

Both the localization of *ABCR* transcripts exclusively within photoreceptor cells and the progressive retinal degeneration caused by mutations of the *ABCR* gene, indicate that ABCR mediates the transport of an essential molecule (or ion) either into or out of photoreceptor cells. The accumulation in the RPE of a lipofuscin-like substance in STGD/FFM further suggests that the site of ABCR-mediated transport may be on the apical face of the photoreceptor cell and that this transport might effect exchange between the RPE and the photoreceptors. The RPE participates in the continual renewal of visual pigments and of photoreceptor outer segments by recycling the 11-*cis* retinal chromophore and by phagocytosing and digesting 10% of each outer segment per day[32]. Thus, on a time scale of days to weeks any material that accumulates in the outer segment is transferred to the RPE as a result of phagocytosis. The efficient recycling of outer segment components between the photoreceptor cells and the RPE is evidenced by the large reduction in visual pigment regeneration that occurs when the retina is isolated from the RPE[33] and by the unique ability of outer segments to maintain their high content of essential polyunsaturated fatty acids following a shift from a normal diet to one deficient in these fatty acids[34].

The best studied molecules that cycle between photoreceptors and the RPE are the retinoids[35]. In the photoreceptor, light activates the visual pigment by photoisomerization of its retinal chromophore from the 11-*cis* to the all-*trans* configuration. On a time scale of minutes, the photoactivated visual pigment is recycled by dissociation of all-*trans* retinal and subsequent reattachment of 11-*cis* retinal. The released all-*trans* retinal is reduced rapidly in the outer segment to all-*trans* retinol, transported to the RPE, enzymatically isomerized to the 11-*cis* configuration, and transported back to the photoreceptor outer segment. As retinol is poorly soluble in water, its transport between the photoreceptor and the RPE is facilitated by binding to the interphotoreceptor retinol binding protein (IRBP), an abundant extracellular protein that is secreted by photoreceptor cells into the subretinal space[36]. If ABCR is involved in either export or import of retinoids, then mutations in ABCR should lead to an accumulation of retinoids or their derivatives in the outer segment or the RPE, respectively.

Outer segment membranes are distinguished from other cell membranes by a high fluidity, a property that appears to be required for efficient diffusional encounters between integral and peripheral membrane proteins involved in phototransduction. This high membrane fluidity results from a lipid composition that is low in cholesterol and extraordinarily high in essential polyunsaturated fatty acids[37]. Another membrane component that is present in the outer segment at unusually high concentration is vitamin E (alpha-tocopherol), which presumably acts to quench photo-oxidation damage, especially among the polyunsaturated fatty acids. Interestingly, vitamin E deficiency in monkeys causes a large accumulation of lipofuscin in the RPE and a localized macular degeneration[38]. In this animal model, lipofuscin accumulation is presumed to result from an inability of the RPE to degrade and/or to recycle peroxidized outer segment lipids. Therefore, based on its site of expression and the pathophysiology of STGD/FFM, ABCR might plausibly be involved in either the recycling of fatty acids or the uptake of vitamin E by photoreceptors.

A number of ABC proteins transport hydrophobic molecules. These include ABC proteins that transport vitamins into bacteria (reviewed in ref.15), fatty acids into peroxisomes in mammals and yeast[15,39,40], and phospholipids across the plasma membrane of mammalian cells[41,42]. If ABCR mediates the recycling of retinoids, lipids, or lipid components such as vitamin E, it is likely to do so in conjunction with specific extracellular and/or intracellular binding proteins, the genes for which would then be candidates for inherited retinopathies. Finally, we note that if ABCR mediates the cycling of outer segment components between the RPE and the retina, then it would be predicted to reside on the apical plasma membrane of the photoreceptor cell, including, perhaps, the outer segment membrane.

ABCR and the pathophysiology of STGD/FFM. The few histopathologic studies of eyes with STGD/FFM show massive accumulation of lysosomal material similar to lipofuscin within RPE cells[43–48]. Other studies of normal and ageing eyes have identified lipofuscin accumulation in the RPE, with greater amounts

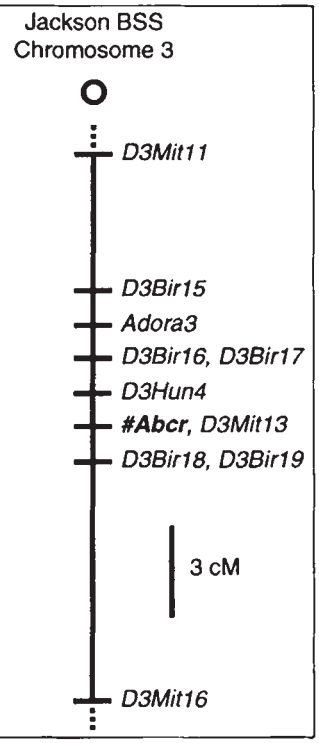

Fig. 5 Location of *Abcr* on mouse chromosome 3. Map from the Jackson BSS Backcross showing a portion of mouse chromosome 3. The map is depicted with the centromere toward the top. A 3-cM scale bar is shown to the right. Loci mapping to the same position are listed in alphabetical order.

accumulating in the posterior pole where the density of adjacent photoreceptors is highest[49,50]. A recent histopathologic and immunocytochemical study of STGD/FFM additionally emphasized abnormal photoreceptor morphology and abnormal accumulation of lipofuscin in photoreceptor inner segments[48]. Thus, the clinical and histopathologic observations of abnormal and premature accumulation of lipofuscin could result from any of a number of principal defects, including: i) accelerated turnover of photoreceptor cells; ii) increased phagocytosis of photoreceptor outer segments; iii) abnormal photoreceptor membranes or contents rendered indigestible by the RPE; iv) missing or mutated degradative enzymes capable of digesting photoreceptor proteins or lipids; or v) failed mechanisms to expel lipofuscin from the cytoplasm of the RPE[46].

The localization of ABCR to rods and its apparent absence from cones is consistent with the widespread distribution of lipofuscin-like material in the retinas of STGD/FFM patients, but is surprising given that the principal symptoms in these patients are referable to cone dysfunction. However, we note that the macular area over which significant functional and anatomic defects are found in STGD/FFM patients extends well beyond the 1-mm diameter zone that encompasses the cone-dominated region of the retina. These data suggest that the macular localization of dysfunction in STGD/FFM may reflect regional differences in susceptibility of the RPE and/or photoreceptors to insult. Specifically, these data are consistent with a model in which cone dysfunction is a consequence of RPE dysfunction which, in turn, is a consequence of the primary lesion within the rods.

We observed a high frequency of missense mutations in the *ABCR* gene in STGD families; in each family in which we identified two mutant alleles at least one of the alleles was a missense change or in-frame deletion. This suggests that most STGD patients may have at least one allele that retains partial function. However, the 15-bp in-frame homozygous deletion identified in family AR293 deletes five amino acids, including a portion of a putative transmembrane domain. It will be interesting to determine if individuals with STGD/FFM or with other retinopathies have alterations that completely disrupt ABCR and whether specific mutations in *ABCR* correlate with the age-of-onset or progression of disease.

ABCR joins a growing and diverse collection of genes that when mutated result in retinal degeneration. The best characterized of these are the genes responsible for some forms of retinitis pigmentosa, a group of recessive, dominant and X-linked disorders that affect photoreceptor function. Mutations responsible for autosomal recessive and/or dominant retinitis pigmentosa have been identified in genes encoding photoreceptor proteins that mediate phototransduction (rhodopsin, cGMP phosphodiesterase, and the cGMP gated channel) or maintain rod outer segment structure (peripherin/RDS and ROM-1) (reviewed in ref. 51). The products of several other retinal disease genes are widely expressed and appear to act at diverse points in the cell biology of the retina and/or the RPE. The gene for one type of X-linked retinitis pigmentosa encodes a protein with homology to guanine nucleotide exchange factors[52]; the choroideraemia gene encodes a geranylgeranyl transferase[53]; the gene encoding ornithine amino transferase is mutated in gyrate atrophy[54]; the gene responsible for Sorsby's fundus dystrophy encodes a tissue inhibitor of metalloproteinase-3 (ref.55); and the Norrie disease gene encodes an extracellular protein of unknown function[56,57].

Implications for other retinopathies. The identification of *ABCR* as the gene responsible for STGD/FFM invites speculation regarding a possible relationship between *ABCR* and other retinopathies, in particular, age-related macular degeneration. Age-related maculopathies share several phenotypic similarities with STGD, including the accumulation of cellular debris (drusen) in and under the retinal pigment epithelium, and the progressive and geographic atrophy of the foveal and macular RPE, with consequent loss of photoreceptor function and resultant impairment of both central acuity and the central visual field. It will be of interest to determine whether the estimated 1% of humans who are heterozygous carriers of *ABCR* mutations have an elevated incidence of mild or late-onset visual disorders. Once the biochemical activity of ABCR is defined, the identification of additional components in the same pathway may reveal fundamental mechanisms of pathogenesis of both photoreceptor and pigment epithelial disease. Finally, the possibility exists that STGD/FFM, and perhaps other retinopathies, might be treatable with compounds that act on ABCR or the pathway in which it functions.

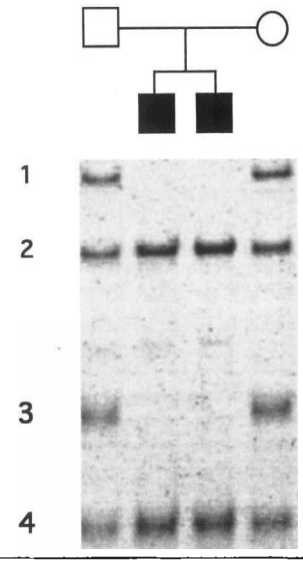

Fig. 6 Segregation of SSCP variants in the exon beginning of nucleotide 4905 of the *ABCR* gene in kindred AR293. Sequence analysis of SSCP bands revealed the existence of wild-type sequence (bands 1 and 3) and mutant sequence (bands 2 and 4). DNA sequencing revealed a 15-bp deletion in the aberrant bands. Parents are heterozygous for the in-frame 15-bp deletion, while the affected children (lanes 2 and 3) are homozygous. Haplotype analysis demonstrated homozygosity at the *STGD* locus in the two affected individuals (data not shown).

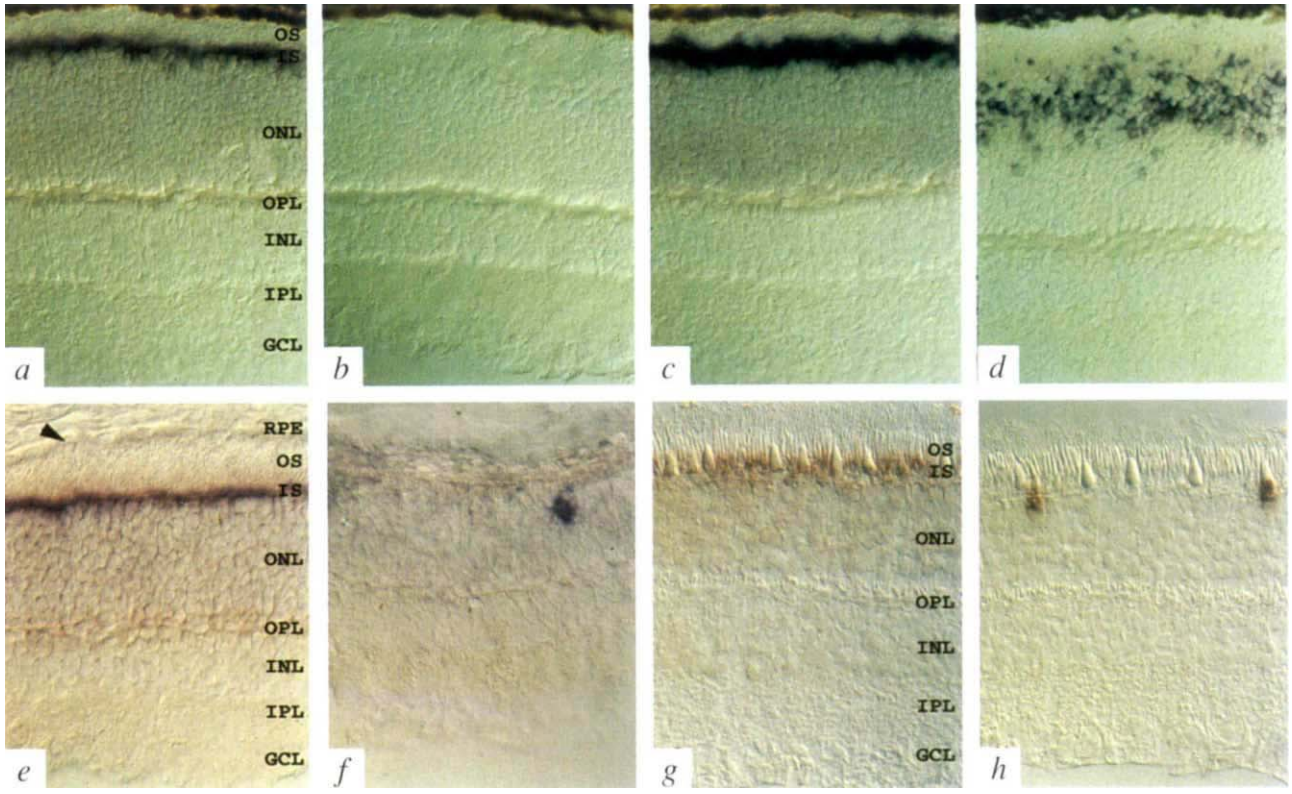

Fig. 7 Localization of *ABCR* transcripts to photoreceptor cells. *In situ* hybridization was performed with digoxygenin-labelled riboprobes and visualized using an alkaline phosphatase conjugated anti-digoxygenin antibody. ***a-d***, Retina and choroid from a pigmented mouse (C57/Bl6); ***e***, ***f***, Retina and choroid from an albino rat; ***g***, ***h***, Retina from a macaque monkey. ***a***, ***e***, ***g***, Mouse *abcr* antisense probe; ***b***, Mouse *abcr* sense probe; ***c***, Macaque rhodopsin antisense probe; ***d***, ***f***, ***h***, Mouse blue cone pigment antisense probe. *ABCR* transcripts are localized to the inner segments of the photoreceptor cell layer, a pattern that matches the distribution of rhodopsin transcripts but is distinct from the distribution of cone visual pigment transcripts. Hybridization is not observed in the RPE or choroid, as seen most clearly in the albino rat eye (arrowhead in (*e*)). The retinal layers indicated in (*b*) are: OS, outer segments; IS, inner segments; ONL, outer nuclear layer; OPL, outer plexiform layer; INL, inner nuclear layer; IPL, inner plexiform layer; GCL, ganglion cell layer.

Methods

STGD patients. Forty-five North American and three Saudi Arabian families with STGD/FFM were examined in this study. Among these, at least four were consanguineous families in which the parents were first cousins. Entry criteria for the characterization of the clinical and angiographic diagnosis of Stargardt disease, ascertainment of the families and methods of their collection, including the consanguineous families from Saudi Arabia, are as described[4,30].

Sequence analysis. Searches of the dbEST[58] database were performed with BLAST on the NCBI file service[59]. Amino-acid alignments were generated with PILEUP[60]. Sequences were analysed with programs of the Genetics Computer Group package[61] on a VAX computer.

Genomic and cDNA cloning. cDNA clones containing *ABCR* sequences were obtained from a human retina cDNA library[62] and fully sequenced. Primers were designed from the sequences of cDNA clones from 5' and 3' regions of the gene and used to link the identified cDNA clones by RT-PCR with retina QUICK-Clone cDNA (Clontech) as a template. PCR products were cloned into pGEM-T vector (Promega). Mouse *ABCR* cDNA clones were obtained from screening a developing mouse eye cDNA library (H.S., A. Lanahan, and J.N., unpublished). cDNA clones from various regions of the *ABCR* gene were used as probes to screen a human genomic library in λ FIX II (#946203, Stratagene).

Exon/intron structure of the human *ABCR* gene. Primers for the cDNA sequences of the *ABCR* were designed with the PRIMER program[63]. Both *ABCR* cDNA clones and genomic clones were used as templates for sequencing. Sequencing was performed with the *Taq* dye-deoxy terminator cycle sequencing kit (Applied Biosystems), according to the manufacturer's instructions. Sequencing reactions were resolved on an ABI 373A automated sequencer. Positions of introns were determined by comparison between genomic and cDNA sequences. Primers for amplification of individual exons were designed from adjacent intron sequences 20–50 bp from the splice site. Amplification of exons was performed with AmpliTaq gold polymerase in a 25 µl volume in 1× PCR buffer supplied by the manufacturer (Perkin Elmer). Samples were heated to 95 °C for 10 min and amplified for 35–40 cycles of 96 °C, 20 s; 58 °C, 30 s; 72 °C, 30 s. PCR products were analysed on 1–1.5% agarose gels and in some cases digested with an appropriate restriction enzyme to verify their sequence. Primer sequences and specific reaction conditions are available upon request. The sequence of the *ABCR* cDNA has been deposited with GenBank under accession U88667.

Northern hybridization. DNA fragments used as probes were purified on a 1% low-melting temperature agarose gel. DNA was labelled directly in agarose with the Random primed DNA labelling kit (Boehringer) and hybridized to a multiple tissue northern blot and a Master blot (Clontech), according to the manufacturer's instructions. Each blot contains 2 µg of poly(A)$^+$ RNA from various human tissues. Total RNA was isolated from adult rat tissues using the guanidinium thiocyanate method[64] and resolved by agarose gel electrophoresis in the presence of formaldehyde[65]. Hybridization with the mouse *ABCR* probe was performed in 50% formamide, 5X SSC at 42 °C, and filters were washed in 0.1X SSC at 68 °C.

Mutation detection. Mutations were detected by a combined SSCP[66] and heteroduplex analysis[67] under optimized conditions[68]. Genomic DNA samples (50 ng) were amplified with AmpliTaq gold polymerase in 1X PCR buffer supplied by the manufacturer (Perkin Elmer) containing [α-^{32}P] dCTP. Samples were heated to 95 °C for 10 min and amplified for 35–40 cycles of 96 °C, 20 s; 58 °C, 30 s; 72 °C, 30 s. Products were diluted in 1:3 stop solution, denatured at 95 °C for 5 min, chilled in ice

for 5 min, and loaded on gels. Gel formulations include 6% acrylamide:Bis (2.6% cross-linking), 10% glycerol at room temperature, 12 W; and 10% acrylamide:Bis (1.5% cross-linking), at 4 °C, 70 W. Gels were run for 2–16 h (3000 Vh/100 bp), dried, and exposed to X-ray film for 2–12 h. Some exons were analysed by SSCP with MDE acrylamide (FMC) with and without 10% glycerol for 18 h, 4 W at room temperature with [α-P^{33}]-dCTP labelled DNA. Heteroduplexes were identified from the double-stranded DNA at the bottom of the gels and SSCPs were identified from the single-stranded region. Samples showing variation were compared with other family members to assess segregation of the alleles and with at least 40 unrelated control samples, from either Caucasian or Saudi Arabian populations, to distinguish mutations from polymorphisms unrelated to STGD. PCR products with SSCP or heteroduplex variants were obtained in a 25-μl volume, separated on a 1% agarose gel, and isolated by a DNA purification kit (Jetsorb, Genomed). Sequencing was performed on an ABI sequencer with both dye primer and dye terminator chemistry.

Some mutations were identified with a heteroduplex analysis protocol[69]. Equimolar amounts of control and patient PCR products were mixed in 0.2 ml tubes. Two volumes of PCR product from a normal individual served as a negative control, and *MPZ* exon 3 from patient BAB731 as a positive control[70]. Samples were denatured at 95 °C for 2 min and cooled to 35 °C at a rate of 1 °C/min. Samples were loaded onto 1.0-mm thick, 40-cm MDE gels (FMC Bioproducts), electrophoresed at 600–800 V for 15–20 h, and visualized with ethidium bromide. Samples showing a variant band were reamplified with biotinylated forward and reverse primers and immobilized on streptavidin-conjugated beads[71]. The resulting single strands were sequenced by the dideoxy-sequencing method with Sequenase 2.0 (United States Biochemicals).

Mapping of the mouse *abcr* gene. Clones corresponding to the mouse orthologue of the human *ABCR* gene were isolated from the mouse retina cDNA library and end-sequenced. The chromosomal location of the mouse *ABCR* gene was determined on The Jackson Laboratory (Bar Harbor, ME) interspecific backcross mapping panel (C57BL/6JEi X SPRET/Ei)F1 X SPRET/Ei[72], known as Jackson BSS. Mapping was performed by SSCP analysis with the primers MABCR1F 5'–ATC CAT ACC CTT CCC ACT CC–3' and MABCR1R 5'–GCA GCA GAA GAT AAG CAC ACC–3'. PCR reactions and acrylamide gel electrophoresis conditions are as described above. The allele pattern of the *Abcr* was compared to the other 2,450 loci mapped in the Jackson BSS cross (http://www.jax.org).

***In situ* hybridization.** *In situ* hybridization with digoxigenin-labelled riboprobes has been described[73]. For mouse and rat, unfixed whole eyes were frozen and sectioned; macaque retinas were obtained following cardiac perfusion with paraformaldehyde as described[74]. An extra incubation of 30 min in 1% Triton X-100, 1× PBS was applied to the fixed monkey retina sections immediately after the acetylation step. The templates for probe synthesis were: (i) a 1.6-kb fragment encompassing the 3' end of the mouse *Abcr* coding region, (ii) a full length cDNA clone encoding the mouse blue cone pigment[75], and (iii) a macaque rhodopsin-coding-region segment encoding residues 133 to 254.

GenBank accession numbers. *ABCR* cDNA: U88667.

Acknowledgements

We thank participating families and their attending physicians. We thank S. Cevario, C. Riley, C. Davenport, J. Ptak, and M. Kazienko for oligonucleotide synthesis and assistance with DNA sequencing; M. Hanson, M. Barter and L. Rowe for assistance with the mouse mapping; S. Hendry and H. Zhou for a gift of macaque retina; the Baylor YAC core facility; the University of Utah Health Sciences Sequencing Facility (supported in part by NCI grant #5P30CA42014). Computing resources were provided by the Frederick Biomedical Supercomputing Center. This study has been supported in part by grants from The Foundation Fighting Blindness (K.L.A., L.B., R.A.L., J.R.L., J.N.), Research To Prevent Blindness (R.A.L.), the Steinbach Fund (J.R.L., R.A.L., J.N.), the W.M. Keck foundation (A.P., M.L), and the Tornquist Charitable Foundation (M.L.). R.A.L. is a Research To Prevent Blindness Senior Scientific Investigator. J.N. is a Howard Hughes Medical Institute investigator. Support for N.F.S. is from a National Eye Institute, National Institutes of Health pre-doctoral training grant; for K.L.A. is from the NIH Medical Scientist Training Program and the National Eye Institute predoctoral training grant at Baylor College of Medicine. The content of this publication does not necessarily reflect the views or policies of the Department of Health and Human Services, nor does mention of trade names, commercial products, or organizations imply endorsement by the U.S. Government.

Received 8 January; accepted 6 February 1997.

1. National Advisory Eye Council. *Vision Research, a National Plan, 1994-1998.* National Institutes of Health publication 93-3186 (1993).
2. Blacharski, P.A. Fundus flavimaculatus. in *Retinal dystrophies and degenerations,* (ed. Newsome, D.A.) 135–159 (New York: Raven Press, 1988).
3. Stargardt, K. Über familiäre, progressive degeneration in der maculagegend des auges. *Albrecht von Graefes Arch. Klin. Exp. Ophthalmol.* **71**, 534–550 (1909)
4. Anderson, K.L. *et al.* A YAC contig encompassing the recessive Stargardt disease gene (*STGD*) on chromosome 1p. *Am. J. Hum. Genet.* **57**, 1351–1363 (1995).
5. Franceschetti, A. Über tapeto-retinale degenerationen im kindesalter. in *Entwicklung und fortschritt in der augenheilkunde.* (ed von Sautter, H.) 107–120 (Stuttgart: Ferdinand Enke, 1963).
6. Fishman, G.A. Fundus flavimaculatus: a clinical classification. *Arch. Ophthalmol.* **94**, 2061–2067 (1976).
7. Noble, K.G. & Carr, R.E. Stargardt's disease and fundus flavimaculatus. *Arch. Ophthalmol.* **97**, 1281-1285 (1979).
8. Kaplan, J. *et al.* A gene for Stargardt's disease (*fundus flavimaculatus*) maps to the short arm of chromosome 1. *Nature Genet.* **5**, 308–311 (1993).
9. Gerber, S. *et al.* A gene for late-onset fundus flavimaculatus with macular dystrophy maps to chromosome 1p13. *Am. J. Hum. Genet.* **56**, 396–399 (1995).
10. Hoyng, C.B. *et al.* Genetic fine mapping of the gene for recessive Stargardt disease. *Hum. Genet.* **98**, 500–504 (1996).
11. Zhang, K. *et al.* A dominant Stargardt's macular dystrophy locus maps to chromosome 13q34. *Arch. Ophthalmol.* **112**, 759–764 (1994).
12. Stone, E.M. *et al.* Clinical features of a Stargardt-like dominant progressive macular dystrophy with genetic linkage to chromosome 6q. *Arch. Ophthalmol.* **112**, 765–772 (1994).
13. Gass, J.D.M. Stargardt's disease (Fundus Flavimaculatus). in *Stereoscopic atlas of macular diseases: diagnosis and treatment* (ed. Gass, J.D.M.) 256–261 (St Louis, Missouri: C.V. Mosby, 1987).
14. Childs, S. & Ling, V. The MDR superfamily of genes and its biological implications. in *Important advances in oncology* (eds V.T. DeVita, S. Hellman, S. & Rosenberg, S.A.) 21–36 (Philadelphia, Pennsylvania: Lippincott Company, 1994).
15. Dean, M. & Allikmets, R. Evolution of ATP-binding cassette transporter genes. *Curr. Opin. Genet. Dev.* **5**, 779–785 (1995).
16. Riordan, J.R. *et al.* Identification of the cystic fibrosis gene: cloning and characterization of complementary DNA. *Science* **245**, 1066–1073 (1989).
17. Mosser, J. *et al.* Putative X-linked adrenoleukodystrophy gene shares unexpected homology with ABC transporters. *Nature* **361**, 726–730 (1993).
18. Thomas, P.M. *et al.* Mutations in the sulfonylurea receptor gene in familial persistent hyperinsulinemic hypoglycemia of infancy. *Science* **268**, 426–429 (1995).
19. Shimozawa, N. *et al.* A human gene responsible for Zellweger syndrome that affects peroxisome assembly. *Science* **255**, 1132–1134 (1992).
20. de la Salle, H. *et al.* Homozygous human TAP peptide transporter mutation in HLA class I deficiency. *Science* **265**, 237–241 (1994).
21. Hyde, S.C. *et al.* Structural model of ATP-binding proteins associated with cystic fibrosis, multidrug resistance and bacterial transport. *Nature* **346**, 362–365 (1990).
22. Michaelis, S. & Berkower, C. Sequence comparison of yeast ATP binding casette (ABC) proteins. in *Cold Spring Harbor Symposium on Quantitative Biology,* vol.LX: *Protein kinesis - the dynamics of protein trafficking and stability.* (Cold Spring Harbor Laboratory Press, Cold Spring Harbor, New York, 1995).
23. Allikmets, R., Gerrard, B., Court, D. & Dean, M. Cloning and organization of the *abc* and *mdl* genes of *Escherichia coli*: relationship to eukaryotic multidrug resistance. *Gene* **136**, 231–236 (1993).
24. Allikmets, R. *et al.* Characterization and mapping of three new mammalian ATP-binding transporter genes from an EST database. *Mamm. Genome* **6**, 114—117 (1995).
25. Dean, M. *et al.* Mapping and sequencing of two yeast genes belonging to the ATP-binding cassette superfamily. *Yeast* **10**, 377–383 (1994).
26. Luciani, M.-F., Denizot, F., Savary, S., Mattei, M.G. & Chimini, G. Cloning of two novel ABC transporters mapping on human chromosome 9. *Genomics* **21**, 150–159 (1994).
27. Allikmets, R., Gerrard, B., Hutchinson, A. & Dean, M. Characterization of the human ABC superfamily: Isolation and mapping of 21 new genes using the expressed sequence tags database. *Hum. Mol. Genet.* **5**, 1649–1655 (1996).
28. Lennon, G., Auffray, C., Polymeropoulos, M. & Soares, M.B. The I.M.A.G.E. consortium: An integrated molecular analysis of genomes and their expression. *Genomics* **33**, 151–152 (1996).
29. Klugbauer, N. & Hofmann, F. Primary structure of a novel ABC transporter with a chromosomal localization on the band encoding the multidrug resistance-associated protein. *FEBS Lett.* **391**, 61–65 (1996).
30. Anderson, K.L. Towards the isolation of genes recessively inherited ocular disorders. Ph.D. thesis. Baylor College of Medicine (1996).
31. Luciani, M.-F. & Chimini, G. The ATP binding cassette transporter ABC1, is required for the engulfment of corpses generated by apoptotic cell death. *EMBO J.* **15**, 226–235 (1996).
32. Zinn, K.M. & Marmor, M.F. The retinal pigment epithelium. 521 (Harvard University Press, Cambridge. MA, 1979).
33. Dowling, J.E. Chemistry of visual adaptation in the rat. *Nature* **188**, 114–118 (1960).
34. Anderson, R.E. & Maude, M.B. Lipids of ocular tissues: the effects of essential fatty acid deficiency on the phospholipids of the photoreceptor membranes of rat retina. *Arch. Biochem. Biophys.* **151**, 270–276 (1971).
35. Rando, R.R. The chemistry of vitamin A and vision. *Angew. Chem. Int. Ed. Engl.* **29**, 461–480 (1990).
36. Fong, S.-L., Liou, G.I., Landers, R.A., Alvarez, R.A. & Bridges, C.D. Purification and characterization of a retinol-binding glycoprotein synthesized and secreted by bovine neural retina. *J. Biol. Chem.* **259**, 6534–6542 (1984).
37. Daemen, F.J.M. Vertebrate rod outer segment membranes. *Biochem.Biophys. Acta* **300**, 255–288 (1973).
38. Hayes, K.C. Retinal degeneration in monkeys induced by deficiencies of vitamin E or A. *Invest. Ophthalmol.* **13**, 499–510, (1974).
39. Hettema, E.H. *et al.* The ABC transporter proteins Pat1 and Pat2 are required for import of long-chain fatty acids into peroxisomes of *Saccharomyces cerevisiae. EMBO J.* **15**, 3813–3822 (1996).
40. Shani, N. & Valle, D. A *Saccharomyces cerevisiae* homolog of the human adrenoleukodystrophy transporter is a heterodimer of two half ATP-binding cassette transporters. *Proc. Natl. Acad. Sci. USA* **93**, 11901–11906 (1996).
41. Smit, J.J.M. *et al.* Homozygous disruption of the murine mdr2 P-glycoprotein gene leads to a complete absence of phospholipid from bile and to liver disease. *Cell* **75**, 451–462 (1993).
42. van Helvoort, A. *et al.* MDR1 P-glycoprotein is a lipid translocase of broad specificity, while MDR3 P-glycoprotein specifically translocates phosphatidylcholine. *Cell* **87**, 507–517 (1996).
43. Klein, B.A. & Krill, A.E. Fundus Flavimaculatus: clinical, functional, and histopathologic observations. *Am. J. Ophthalmol.* **64**, 3–23 (1967).
44. Eagle, R.C. Jr., Lucier, A.C., Bernadino, V.B. Jr. & Yanoff, M. Retinal pigment epithelial abnormalities in *Fundus Flavimaculatus*: A light and electron microscopic study. *Ophthalmology* **87**, 1189–1200 (1980).
45. McDonnell, P.J., Kivlin, J.D., Maumenee, I.H. & Green, W.R. Fundus flavimaculatus without maculopathy: a clinicopathologic study. *Ophthalmology* **93**, 116–119 (1986).
46. Lopez, P.F., Maumenee, I.H., de la Cruz, Z. & Green, W.R. Autosomal-dominant fundus flavimaculatus: clinicopathologic correlation. *Ophthalmology* **97**, 798–809 (1990).
47. Steinmetz, R.L., Garner, A., Maguire, J.I. & Bird, A.C. Histopathology of incipient fundus flavimaculatus. *Ophthalmology* **98**, 953–956 (1991).
48. Birnbach, C.D., Järveläinen, M., Possin, D.E. & Milam, A.H. Histopathology and immunocytochemistry of the neurosensory retina in fundus flavimaculatus. *Ophthalmology* **101**, 1211–1219 (1994).
49. Wing, G.L., Blanchard, G.C. & Weiter, J.J. The topography and age relationship of lipofuscin concentration in the retinal pigment epithelium. *Invest. Ophthalmol. Vis. Sci.* **17**, 601–607 (1978).
50. Weiter, J.J., Delori, F.C., Wing, G.L. & Fitch, K.A. Retinal pigment epithelial lipofuscin and melanin and choroidal melanin in human eyes. *Invest. Ophthalmol. Vis. Sci.* **27**, 145–152 (1986).
51. Dryja, T.P. & Li, T. Molecular genetics of retinitis pigmentosa. *Hum. Mol. Genet.* **4**, 1739–1743 (1995).
52. Meindl, A. *et al.* A gene (*RPGR*) with homology to the *RCC1* guanine nucleotide exchange factor is mutated in X-linked retinitis pigmentosa (RP3). *Nature Genet.* **13**, 35–42 (1996).
53. Seabra, M.C., Brown, M.S. & Goldstein, J.L. Retinal degeneration in choroideremia: deficiency of Rab geranylgeranyl transferase. *Science* **259**, 377–381 (1993).
54. Valle, D. & Simell, O. The hyperornithinemias. in *The metabolic and molecular basis of inherited disease* (eds Scriver, C.R., Beaudet, A.L., Sly, W.S. & Valle, D.) 1147–1185 (McGraw Hill, New York, 1995).
55. Weber, B.H.F., Vogt, G., Pruett, R.C., Stohr, H. & Felbor, U. Mutations in the tissue inhibitor of metalloproteinase-3 (TIMP3) in patients with Sorsby's fundus dystrophy. *Nature Genet.* **8**, 352–355 (1994).
56. Meindl, A. *et al.* Norrie disease is caused by mutations in an extracellular protein resembling the c-terminal globular domain of mucins. *Nature Genet.* **2**, 139–143 (1992).
57. Meitinger, T. *et al.* Molecular modelling of the Norrie disease protein predicts a cystine knot growth factor tertiary structure. *Nature Genet.* **5**, 376–380 (1993).
58. Boguski, M.S., Lowe, T.M. & Tolstoshev, C.M. dbEST-database for 'expressed sequence tags'. *Nature Genet.* **4**, 332–333 (1993).
59. Altschul, S.F., Gish, W., Miller, W., Myers, E.W. & Lipman, D.J. Basic local alignment search tool. *J. Mol. Biol.* **215**, 403–410 (1990).
60. Feng, D.-F. & Doolittle, R.F. Progressive sequence alignment as a prerequisite to correct phylogenetic trees. *J. Mol. Evol.* **25**, 351–360 (1987).
61. Devereaux, J., Haeberli, P. & Smithies, O. A comprehensive set of sequence analysis programs for the VAX. *Nucl. Acids Res.* **12**, 387–395 (1984).
62. Nathans, J., Thomas, D. & Hogness, D.S. Molecular genetics of human color vision: the genes encoding blue, green, and red pigments. *Science* **232**, 193–202 (1986).
63. Lincoln, A.L., Daly, M. & Lander, E. PRIMER: a computer program for automatically selecting PCR primers. Whitehead Institute Technical Report (1991).
64. Chomczynski, P. & Sacchi, N. Single-step method of RNA isolation by acid guanidinium thiocyanate-phenol-chloroform extraction. *Anal. Biochem.* **162**, 156–159 (1987).
65. Sambrook, J., Fritsch, E.F. & Maniatis, T. Molecular Cloning. (Cold Spring Harbor Laboratory press, New York, 1989).
66. Orita, M., Suzuki, Y., Sekiya, T. & Hayashi, K. Rapid and sensitive detection of point mutations and DNA polymorphisms using the polymerase chain reaction. *Genomics* **5**, 874–879 (1989).
67. White, M., Carvalho, M., Derse, D., O'Brien, S.J. & Dean, M. Detecting single base substitutions as heteroduplex polymorphisms. *Genomics* **12**, 301–306 (1992).
68. Glavač, D. & Dean, M. Optimization of the single strand conformation polymorphism (SSCP) technique for detection of point mutations. *Hum. Mutat.* **2**, 404–414 (1993).
69. Roa, B.B. *et al.* Charcot-Marie-Tooth disease type 1A, association with a spontaneous point mutation in the *PMP22* gene. *New Engl. J. Med.* **329**, 96–101 (1993).
70. Roa, B.B. *et al.* Myelin protein zero (*MPZ*) gene mutations in nonduplication type 1 Charcot- Marie-Tooth disease. *Hum. Mut.* **7**, 36–45 (1996).
71. Warner, L.E. *et al.* Clinical phenotypes of different *MPZ* (P_0) mutations may include Charcot-Marie-Tooth type 1B, Dejerine-Sottas, and congenital hypomyelination. *Neuron* **17**, 451–460 (1996).
72. Rowe, L.B. *et al.* Maps from two interspecific backcross DNA panels available as a community genetic mapping resource. *Mamm. Genome* **5**, 253–274 (1994).
73. Schaeren-Wiemers, N. & Gerfin-Moser, A. A single protocol to detect transcripts of various types and expression levels in neural tissue and culture cells: in situ hybridization using digoxigenin-labelled cRNA probes. *Histochemistry* **100**, 431–440 (1993).
74. Zhou, H., Yoshioka, T. & Nathans, J. Retina-derived POU-domain factor-1: a complex POU-domain gene implicated in the development of retinal ganglion and amacrine cells. *J. Neurosci.* **16**, 2261–2274 (1996).
75. Chiu, M. I., Zack, D.J., Wang, Y. & Nathans, J. Murine and bovine blue cone pigment genes: cloning and characterization of two new members of the S family of visual pigments. *Genomics* **21**, 440–443 (1994).
76. Bellanne-Chantelot, C. *et al.* Mapping the whole human genome by fingerprinting yeast artificial chromosomes. *Cell* **70**, 1059–1068 (1992).
77. Kuwano, Y., Nakanishi, O., Nabeshima, Y.-I., Tanaka, T. & Ogata, K. Molecular cloning and nucleotide sequence of DNA complementary to rat ribosomal protein S26 messenger RNA. *J. Biochem. (Tokyo)* **97**, 983–992 (1985).